

SIZE EFFECT ON SHEAR STRENGTH OF RC BEAMS USING HSC WITHOUT SHEAR REINFORCEMENT

(Translation from Proceedings of JSCE, Vol.711/V-56, August 2002)



Manabu FUJITA



Ryoichi SATO



Kaori MATSUMOTO



Yasuhiro TAKAKI

The shear strength of reinforced concrete (RC) beams without shear reinforcement is experimentally investigated, with compressive strength and effective depth taken as the major experimental factors. The experiment demonstrates that the size effect is more prominent in high-strength concrete (HSC) than in normal-strength concrete beams. It is also shown that the nominal shear stress normalized by concrete tensile strength at diagonal cracking is proportional to the minus 1/2 power of the ratio of effective depth to characteristic length. Based on this relationship, a new empirical equation is proposed for calculating the shear strength of RC beams without shear reinforcement when made with HSC of compressive strength of 80 - 125 N/mm².

Keywords : high-strength concrete, size effect, shear strength, fracture mechanics

Manabu Fujita is a chief research engineer of Institute of Technology & Development at Sumitomo Construction Co., Ltd. , Japan. He received his Dr. Eng. degree from Hiroshima University in 2002. His research interests are related to prestressed concrete structures. He is a member of JSCE and JCI.

Ryoichi Sato is a professor of Department of Social and Environmental Engineering, Graduate School of Engineering, Hiroshima University. He received his Dr. Eng. degree from Tokyo Institute of Technology in 1982. His research interests are related to mechanical properties of concrete structures. He is a member of JSCE and JCI.

Kaori Matsumoto is research engineer of Institute of Technology & Development at Sumitomo Construction Co., Ltd. , Japan. Her research interests are related to t of prestressed concrete structures. She is a member of JSCE and JCI.

Yasuhiro Takaki is a research engineer of Institute of Technology & Development at Sumitomo Construction Co., Ltd. , Japan. His research interests are related to prestressed concrete structures. He is a member of JSCE and JCI.

1. INTRODUCTION

In recent years, concrete of ever greater strength has become available. The Standard Specification for Design and Construction of Concrete Structures, published by the Japan Society of Civil Engineers (JSCE), already includes concrete with a design standard strength of $f'_{ck} = 80 \text{ N/mm}^2$. Among factory produced concrete items, there are already many examples of high-strength concrete being used, such as in precast members for large-scale concrete bridges and the like. High-strength concrete has excellent durability and enables member cross sections to be reduced, and it also offers the potential for greater to help structural functionality, reduced costs, and other advantages in future design systems that incorporate performance based design. Accordingly, the range of applications of high-strength concrete is expected to increase. Nevertheless, in the interests of designing members that fully utilize the special characteristics of high-strength concrete, it is necessary to gain a thorough understanding of failure modes and load-carrying properties in addition to determining material and dynamic characteristics. Failure mechanisms and size effects in the high-strength domain are largely unknown, particularly for shear strength, and there is a pressing need to elucidate these matters and establish calculation formulas.

Regarding shear strength calculations for reinforced concrete beam members without shear reinforcement, research thus far both in both Japan and abroad has focused on empirical laws or fracture energy properties based on experimental results. In Japan, the aforementioned JSCE Standard Specification for Design and Construction of Concrete Structures [1] contains a calculation (the "JSCE formula"). This calculation is based on a formula proposed by Niwa et al. [2] and derived through analysis and regression of existing experimental results. It takes into account the effect of compressive strength, member size, tensile reinforcement ratio and axial strength, as well as a size effect corresponding to the effective depth to the minus 1/4 power. Nevertheless, the data used to obtain this formula, was limited to a comparatively narrow range of compressive strength, so the JSCE formula is limited to applications where $f'_{ck} \leq 80 \text{ N/mm}^2$. Within this range, the results of FEM analysis carried out using fracture mechanics techniques have been used by, Hillerborg et al. to propose d/l_{ch} to the minus 1/4 power, using effective depth d and characteristic length l_{ch} for the size effect of shear strength of ordinary concrete beams [3].

On the other hand, although research into the shear fracture of high-strength concrete (HSC) members has been progressing in recent years, the quantity of data accumulated is not very great. In order to increase the application of HSC to actual structures, the size effect on the shear strength for HSC must be identified and design equations based on this size effect will be needed.

Previously, the authors have conducted shear tests on reinforced concrete simple beams without shear reinforcement with the aim of determining the effect of concrete strength and the effect of member size on the shear fracture characteristics of RC beam members. In this work, f'_c effective depth d , and the ratio of shear span a to the effective depth d ("the shear span ratio, a/d ") were adopted as parameters [4][5][6]. The results of these tests confirmed that shear fracture in HSC was characterized by conspicuous localization of cracking as compared to ordinary-strength concrete, and that the propagation of these cracks was rapid, resulting in more brittle fracturing. Since the localization of cracking results from tension softening of the concrete, a study using fracture mechanics was conducted to determine the size effect on nominal shear stress intensity (the "shear strength") when diagonal cracking occurs, and a new empirical equation for calculating the shear strength of HSC RC beams without shear reinforcement.

2. EXISTING STUDIES AND DESIGNE CODE FORMULAS

The formulas used to calculate the shear strength of RC beams without shear reinforcement have been standardized in Japan by the Japan Society of Civil Engineers (JSCE). Overseas, standards have been set by the American Concrete Institute (ACI), the Comité Euro-International du Béton and the Fédération Internationale de la Précontrainte (CEB-FIP) and other organizations (**Table 1**). Hereafter, these formulas will be referred to as the JSCE formula, the ACI formula and the CEB-FIP formula. Where not otherwise specified, the symbols represent the following:

- τ_c : Shear strength when diagonal cracking occurs (N/mm^2)
- f'_c : Compressive strength of concrete (N/mm^2)
- f_t : Tensile strength of concrete (N/mm^2)

Table 1 Formulas about shear strength for RC beams without shear reinforcement

	Existing formulas	Range of application
JSCE (1996) [1]	$\tau_c = 0.2 \cdot \sqrt[3]{f'_c} \cdot \sqrt[3]{100 p_w} \cdot \sqrt[4]{1000/d}$ (1)	$0.2 \cdot \sqrt[3]{f'_c} \leq 0.72 \text{ N/mm}^2$ $f'_c \leq 80 \text{ N/mm}^2$
ACI (1999) [7]	$\tau_c = 1.9 \cdot \sqrt{f'_c} + 2500 p_w \cdot V_u \cdot d / M_u$ (2) d : (in), f'_c : (psi) V_u : factored shear force at section considered M_u : factored moment occurring simultaneously	$\tau_c : (\leq 3.5 \sqrt{f'_c})$ (psi) $\sqrt{f'_c} \leq 100 \text{ psi}$
CEB-FIP (1993) [8]	$\tau_c = 0.12 \cdot \sqrt[3]{f'_c} \cdot \sqrt[3]{100 p_w} \cdot (1 + \sqrt{200/d})$ (3)	$f'_c \leq 50 \text{ N/mm}^2$
Niwa et al. [2]	$\tau_c = 0.2 \cdot \sqrt[3]{f'_c} \cdot \sqrt[3]{100 p_w} \cdot \sqrt[4]{1000/d} \cdot [0.75 + 1.4/(a/d)]$ (4)	—
Bazant And Kim [9]	$\tau_c = \frac{8 \cdot \sqrt[3]{p_w} \left(\sqrt{f'_c} + 3000 \sqrt{p_w/(a/d)^5} \right)}{\sqrt{(1 + d/25d_a)}}$ (5) τ_c : (psi), f'_c : (psi), d_a : maximum aggregate size (mm)	—

E_c : Young's modulus of concrete (kN/mm²)

d : Effective depth (mm)

b : Girder width (mm)

a : Shear span (mm)

p_w : Tension reinforcement ratio (= $A_s / (b \times d)$)

A_s : Sectional area of tension side tendons (mm²)

In the JSCE and CEB-FIP formulas, shear strength decreases as effective depth increases; in other words, the size effect is taken into account. In contrast, there is no consideration of size effect in the ACI formula. All of these formulas establish an upper limit for compressive strength and limit the applicable range.

In addition to the standard formulas described above, many other have been proposed for estimating shear. For example, Niwa et al. [2] proposed Eq.(4), the foundation of the JSCE formula, based on research by Okamura and Higai [10] and Iguro et al.. [11].

Investigation of the size effect of shear strength have also been carried out from a fracture mechanics approach. Bazant et al. have proposed a theoretical formula, Eq.(5), based on non-linear fracture mechanics [9]. According to formula [5], the size effect disappears if the maximum aggregate size is proportional to the effective depth. However, it has been reported that this is contradicted by experiments in which aggregate diameter was varied [12]. Hillerborg et al. implemented FEM analysis for RC beams using fracture mechanics techniques and discussed the size effect on shear strength based on the relationship between (a) the ratio τ_c/f_t of shear strength to tensile strength and (b) the ratio d/l_{ch} of the effective depth to the characteristic length l_{ch} (as discussed later); they reported that shear strength is proportional to the minus 1/4 power of effective depth and reported on the effectiveness of fracture mechanics in explaining the size effect on shear strength [3].

The evaluated size effect on shear strength differs among these previous studies. For example, with regard to effective depth, shear strength was noted as being proportional to the minus 1/4 power in Eq.(1) and Eq.(4), and to the minus 1/2 power in Eq.(5). However, almost all of these formulas are based on the results of regression analysis using test data for concrete with a compressive strength $f'_c \leq 50 \text{ N/mm}^2$. In this study, in order to check the prediction accuracy of the existing shear strength estimation formulas with respect to HSC, the upper limit of the applicable compressive strength range has been ignored.

3. OUTLINE OF TEST

Table 2 shows the properties of the test specimens and **Fig.1** is a diagram showing their structure. The various test cases (L, M, and U) represent variations in the strength of the mix. Case L is ordinary-strength concrete ($f'_c = 36 \text{ N/mm}^2$), U represents HSC ($f'_c = 100 \text{ N/mm}^2$), and M is a value mid way between ordinary- and high-strength concrete ($f'_c = 60 \text{ N/mm}^2$). In this test, for each strength level (L, M, and U), two series were established: one designed to examine the size effect, in which the shear span ratio was constant ($a/d = 3$) and the effective depth was varied, and one to examine the effect of shear span ratio, in which the effective depth was constant ($d = 500 \text{ mm}$) and the shear span ratio was varied ($a/d = 2 - 5$).

Table 3 shows the concrete mix proportions for the three strengths. The maximum aggregate size G_{max} was made constant at 20 mm. SD345 was used for the tension reinforcement; the reinforcement was specified as yield strength of 388 N/mm^2 , a tensile strength of 555 N/mm^2 , and a modulus of elasticity of 196 N/mm^2 . The tension reinforcement ratio and the ratio of the sum of the tensile diameters D to the beam width ($= \sum D/b$) were set to almost exactly the same values for each test specimen. The tension reinforcing bars were anchored with right-angle hooks attached to the ends. No shear reinforcement was provided; the ends of the beams were simply provided with stirrups to prevent pull out of the tension reinforcement at failure.

Two-point concentrated static loading was carried out. The load was increased in monotone fashion until fracture. The equimomental section length was made equal to the effective depth. One test specimen was tested for the case with $a/d = 5$ and three for each of the other cases, for a total of 48.

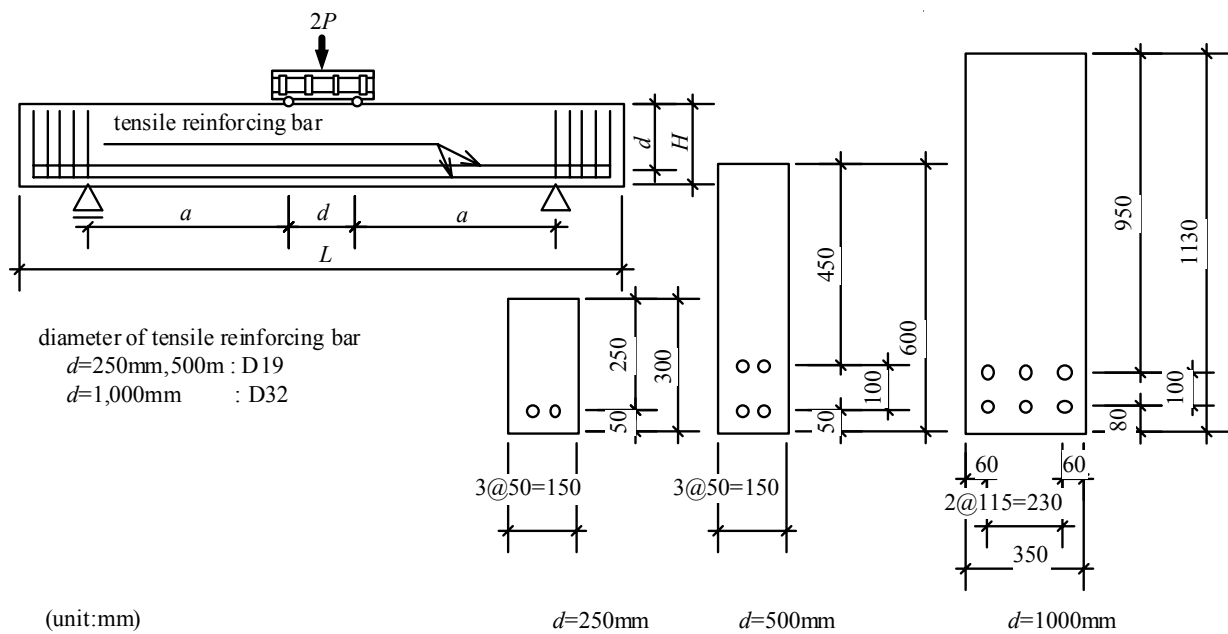


Fig.1 Specimens geometry and load application

Table 3 Mix proportion of concrete

Case	Require strength (N/mm ²)	W/B (%)	s/a (%)	Unit content (kg/m ³)					Chemical admixture × C (%)
				Water W	Binder B		Aggregate		
					Cement C	Silica fume SF	Sand S	Gravel G	
L	36	56.5	47.9	162	287	0	864	966	1.1
M	60	35.0	46.1	165	471	0	789	948	1.2
U	100	21.0	42.2	160	686	76	618	869	1.8

Table 2 Properties of specimens and test results

Case	L mm	b mm	a mm	d mm	a/d	p_w %	f'_c N/mm ²	f_t N/mm ²	E_c kN/mm ²	τ_c N/mm ²	Form	
Size effect	L-25-3	2750	150	750	250	3	1.53	37.8	3.05	27.9	1.15	DTF
								36.4	2.90	31.6	1.48	DTF
								36.4	2.90	31.6	1.50	DTF
	L-50-3	4500	150	1500	500	3	1.53	37.4	2.95	27.8	1.55	DTF
								36.4	2.90	31.6	1.05	DTF
								36.4	2.90	31.6	1.16	DTF
	L-100-3	9000	350	3000	1000	3	1.36	35.7	2.75	27.1	0.91	DTF
								34.7	2.71	28.7	0.85	DTF
								33.7	3.16	28.7	0.95	DTF
	M-25-3	2750	150	750	250	3	1.53	68.8	3.90	37.0	1.37	DTF
								51.9	3.46	29.8	1.74	DTF
								51.9	3.46	29.8	1.43	DTF
	M-50-3	4500	150	1500	500	3	1.53	69.4	3.92	36.3	1.16	DTF
								51.9	3.46	29.8	1.44	DTF
								51.9	3.46	29.8	1.51	DTF
	M-100-3	9000	350	3000	1000	3	1.36	59.2	4.05	31.6	0.90	DTF
								53.7	3.43	33.2	0.97	DTF
								53.0	3.28	33.2	0.97	DTF
	U-25-3	2750	150	750	250	3	1.53	101	4.47	37.8	1.07	DTF
								92.9	4.91	40.8	1.50	DTF
								92.9	4.91	40.8	1.25	DTF
	U-50-3	4500	150	1500	500	3	1.53	102	4.59	37.5	1.15	DTF
								92.9	4.91	40.8	1.10	DTF
								92.9	4.91	40.8	1.30	DTF
	U-100-3	9000	350	3000	1000	3	1.36	103	4.75	39.7	0.80	DTF
								89.8	3.92	36.7	0.75	DTF
								92.1	4.28	36.7	0.80	DTF
Effect of the shear span ratio	L-50-2	3500	150	1000	500	2	1.53	37.2	2.92	27.7	1.33	SCF
								36.4	2.90	31.6	1.30	SCF
								36.4	2.90	31.6	1.39	SCF
	L-50-4	5500	150	2000	500	4	1.53	37.7	3.03	27.9	0.94	DTF
								36.4	2.90	31.6	1.13	DTF
								36.4	2.90	31.6	1.18	DTF
	L-50-5	6500	150	2500	500	5	1.53	37.8	3.04	27.9	-	BF
	M-50-2	3500	150	1000	500	2	1.53	69.3	3.91	36.5	1.31	DTF
								51.9	3.46	29.8	1.63	DTF
								51.9	3.46	29.8	1.53	SCF
	M-50-4	5500	150	2000	500	4	1.53	69.8	3.94	35.8	1.09	DTF
								51.9	3.46	29.8	-	BF
								51.9	3.46	29.8	1.21	DTF
	M-50-5	6500	150	2500	500	5	1.53	70.4	3.76	35.1	-	BF
	U-50-2	3500	150	1000	500	2	1.53	102	4.67	37.3	1.41	DTF
								92.9	4.91	40.8	1.26	DTF
								92.9	4.91	40.8	1.38	SCF
	U-50-4	5500	150	2000	500	4	1.53	101	4.43	37.9	0.97	DTF
								92.9	4.91	40.8	1.05	DTF
								92.9	4.91	40.8	1.12	DTF
	U-50-5	6500	150	2500	500	5	1.53	100	4.38	37.9	-	BF

Note : Results of material tests show data at each experiment.

τ_c take into consideration of weights of specimen and loading device, and cases of $d = 1000$ mm are corrected reinforcement ratio as $p_w = 153$ %.

In this table "form" suggests the form of failure, and "DTF" shows the diagonal tension failure, "SCF" shows the shear compression failure and "BF" shows the bending failure.

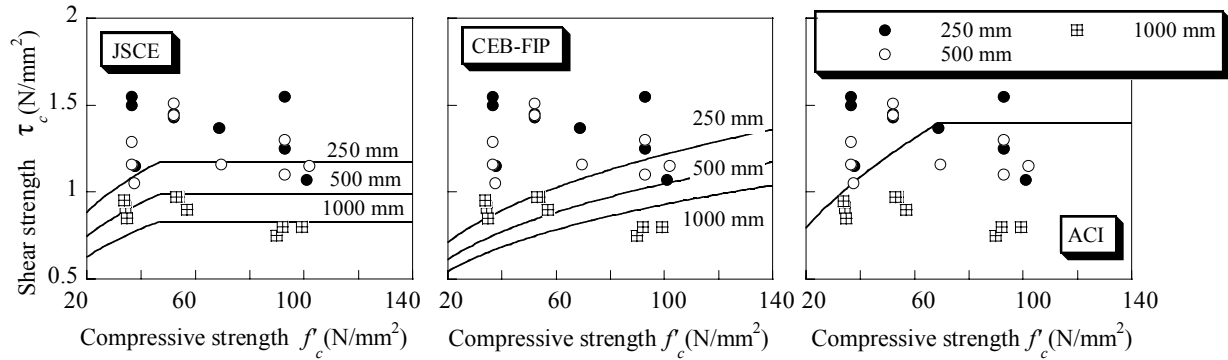


Fig.2 Comparison of design code formulas with test results

4. STUDIES ABOUT FACTORS

Table 2 also shows the test results. In this case of diagonal tension failure and shear compression failure test specimens, the tension reinforcement had not reached the yield strain when diagonal cracking occurred. Moreover, under identical conditions, there was considerable variation in some of the test results, but the reason for this is not clear.

In these tests, the p_w value differed slightly for $d = 1,000$ mm. According to the research done by Suzuki et al., shear strength at the occurrence of diagonal cracking is proportional to $p_w^{1/3}$ for HSC [13]. Based on these findings, the shear strength for $d = 1,000$ mm was multiplied by the offset coefficient $(p_{w0}/p_w)^{1/3}$ for the tension reinforcement ratio and converted to a tension reinforcement ratio of $p_{w0} = 1.53$ % for $d = 250$ mm and 500 mm.

4.1 Comparison of the design code formulas on test results

Figure 2 compares the test results for $a/d=3$ in Table 2 and the shear strength derived using each of the design code formulas given in Section 2. It is clear that the JSCE formula and CEB-FIP formula, both of which take size effect into consideration, offer evaluations that fall in the safe zone for compressive strength value within the range of the design codes, even for cases with an effective depth of 1,000 mm. However, the ACI formula, which did not take size effect into consideration, provided evaluations in the danger zone for the cases with effective depth of 1,000 mm regardless of compressive strength.

With high-strength concrete having a compressive strength of 90 – 100 N/mm², which falls outside the applicable range of the design codes, the JSCE and CEB-FIP formulas offer evaluations that fall slightly inside the danger zone for cases where the effective depth is 1,000 mm. Other cases, however, yield results that remain within the safe zone. The ACI formula yields evaluations in the danger zone for all effective depths, and it is confirmed that the discrepancy between design code formulas and test results is greater for larger effective depths. For each of the design code formulas, the larger the member size, the greater the disparity with the test results and the greater the trend towards evaluations within the danger zone. This latter trend was particularly conspicuous with the ACI formula, which does not consider the size effect.

These results demonstrate that appropriate consideration of the size effect is necessary in order to perform a rational evaluation of shear strength. In particular, it is clear that the shear strength of HSC cannot be properly evaluated using forms of existing design codes.

4.2 Effect of compressive strength on shear strength

Figure 3 shows a comparison of shear strengths derived from Eq.(4) and the test results for cases in Table 2 where the shear span ratio is 3. In order to illustrate the effect of shear strength on concrete strength, the vertical axis is the shear strength τ_c divided by $f_c^{1/3}$, in accordance with Eq.(4). The straight lines in the figure represent the values for effective depth calculated with Eq.(4); they are shown as constant regardless of compressive strength. However, in the test results, the value of $\tau_c / f_c^{1/3}$ is different for each effective

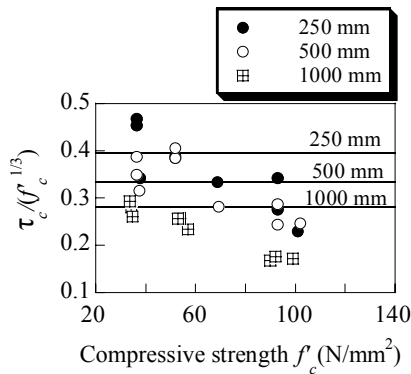


Fig.3 Effect of compressive strength on shear strength

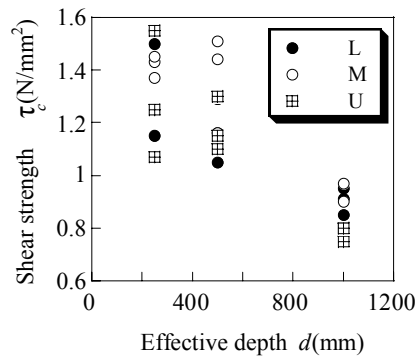


Fig.4 Comparison of effective depth to shear strength

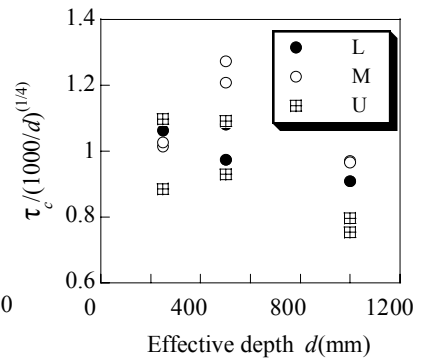


Fig.5 Effect of effective depth on shear strength

depth depending on compressive strength. For compressive strengths exceeding 80 N/mm^2 , there is a clear tendency for shear strength to decrease as compressive strength increases. Accordingly, it is inferred that the relationship between shear strength and compressive strength in high-strength concrete is different from that in ordinary-strength concrete.

4.3 Effect of effective depth on shear strength

Figure 4 shows the relationship between effective depth and the test results for cases in **Table 2** where the shear span ratio is 3. For test specimens of all strength, a greater effective depth means lower shear strength.

In Eq.(4), the size effect is specified as the effective depth to the minus 1/4 power. Based on this, **Fig. 5** shows the relationship between effective depth and the test results, with the shear span ratio given in **Table 2** divided by the effective depth to the minus 1/4 power, $\tau_c / (1000/d)^{1/4}$. Since shear strength is affected by compressive strength, test results for those cases with a shear span ratio of 3, and which exhibited the same degree of compressive strength in each series are shown in the figure. In the U series that corresponds to high-strength concrete, the $\tau_c / (1000/d)^{1/4}$ value for an effective depth of 1,000 mm is significantly lower than the values for the L and M series. This indicates the possibility that the size effect in high-strength concrete may be more marked than specified by effective depth to the minus 1/4 power.

These results confirm that the size effect of shear strength is dependent on compressive strength, and that the size effect is greater in high-strength concrete than in ordinary-strength concrete.

4.4 Relation between shear strength and shear span ratio

In Eq.(4), the effect of shear span ratio on shear strength is taken into account by introducing the $(0.75 + 1.4 / (a/d))$ factor. Hear, to study the effect of shear span ratio on shear strength, the test results in **Table 2** are divided by this factor, $(0.75 + 1.4 / (a/d))$. The study is carried out using data that demonstrates a diagonal tensile failure mode. **Figure 6** shows the relationship between shear span ratio and $\tau_c / (0.75 + 1.4 / (a/d))$. Since the $\tau_c / (0.75 + 1.4 / (a/d))$ values are almost constant, the effect of shear span ratio on shear strength can be evaluated using the shear span ratio factor in Eq.(4) regardless of compressive strength.

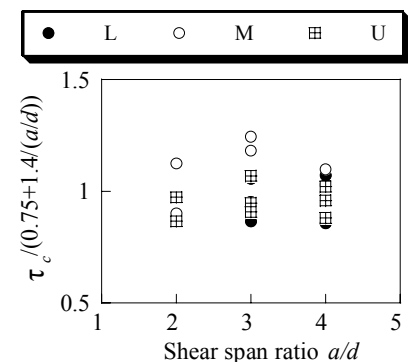


Fig.6 Effect of shear span ratio on shear strength

The above results confirm that, in extending existing design code formulas, evaluations of the shear strength of high-strength concrete fall within the danger zone in some cases for larger effective depths, and that the size effect is greater for high-strength concrete than for ordinary-strength concrete. Further, it is also learned that the relationship between shear strength and shear span ratio is almost constant regardless of compressive strength.

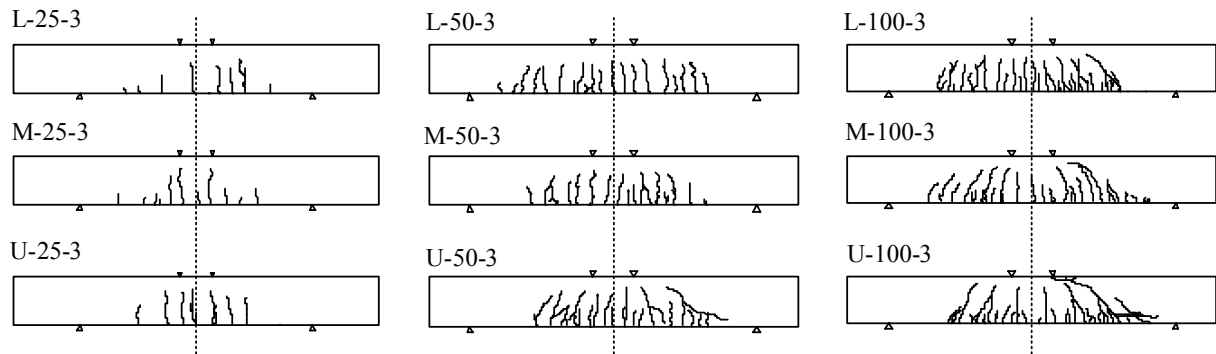


Fig.7 Comparison of crack development at the same nominal shear stress intensity ($\tau = 0.80 \text{ N/mm}^2$)

5. STUDY OF SHEAR STRENGTH OF RC BEAMS USING FRACTURE MECHANICS

In section 4, it was shown that the size effect of shear strength is greater for high-strength concrete than for ordinary-strength concrete. In this section, a fracture mechanics approach to studying the size effect of shear strength is described.

5.1 Characteristics and crack localization

Figure 7 shows the cracking state for each case when the same nominal shear stress intensity is applied, using the shear strength at shear fracturing in U-100-3 as reference. In order to compare the effect of compressive strength and member size on crack propagation, the values are shown on the same scale. Crack localization occurs at a point toward the compression side from the center of the cross-section in each test specimen. The amount of displacement from the center increases with greater effective depths, and is still more significant with greater compressive strengths. This difference in crack localization is thought to be related to shear strength and the size effect on shear strength.

One factor affecting the relationship between effective depth and crack localization is the relative position of the tension reinforcement with respect to the effective depth. It is conjectured that, when the effective depth is greater, the crack distributing effect of the tension reinforcements acts over a relatively smaller range, causing crack localization to become conspicuous at points removed from the reinforcement. The results of analytical research on reinforced concrete beams made of ordinary-concrete without shear reinforcement has shown that beams can be divided into two areas around the tensile reinforcement: one where sufficient tensile stress transmission can be anticipated even after cracking, and a second unreinforced area where sudden tension softening occurs [14] [15]. For the latter, a constitutive law was applied that took softening into account by means of fracture mechanics, and some beams were shown to demonstrate size effect with regard to shear strength.

Conversely, in HSC, the fracture process zone (FPZ) covers a smaller area in ordinary-strength concrete [16]. It is surmised that, in domains other than the FPZ, behavior is almost completely elastic. Consequently, almost all of the elastic energy stored in the test specimen is consumed near the FPZ, which is localized in the domain in front of the crack ends [17], with the result that crack localization becomes even more conspicuous. **Figure 8** compares the load - deflection curves at the center of the span for the L-100-3 and U-100-3 test specimens. The differences in load reduction after maximum load are thought to result from differences in the localization

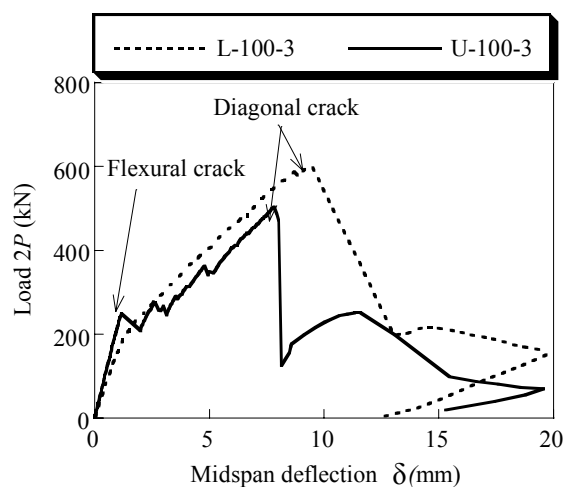


Fig.8 Load-deflection curve with different compressive strengths

Table 4 Results of fracture energy tests

Case	f'_c (N/mm ²)	f_t (N/mm ²)	E_c (kN/mm ²)	γ (g/cm ³)	G_f (N/mm)	l_{ch} (mm)
L	35.1	2.87	29.0	2.28	0.188	661
M	50.2	4.19	32.1	2.34	0.200	366
U	85.6	5.47	37.2	2.40	0.218	271

γ : Concrete density

of cracking. Further, the ratio of initial rigidity in the two test specimens is almost completely in agreement with the Young's modulus ratio obtained from the concrete material tests, so differences in initial rigidity are thought to result from differences in Young's modulus.

As the FPZ develops, it is localized by the tension softening characteristics of the concrete [17]. Additionally, crack localization results from the localization of the FPZ due to tension softening of the concrete. This crack localization becomes more conspicuous with member size, and also with higher compressive. For this reason, it is thought that consideration of concrete tension softening (in other words, the application of fracture mechanics) will lead to more rational evaluations of the size effect on shear strength for HSC.

Several tests and evaluation methods have been proposed for the in-plane shear-type mode II fracture energy. However, at present, fracture energy has not even been clearly defined [16]. On the other hand, tests and evaluations for tensile-type mode I fracture energy have already been drafted by a committee of the Japan Concrete Institute (the Test Method for Fracture Property of Concrete committee) in a document entitled "Test Method for Fracture Energy of Plain Concrete (Draft)" (referred to hereafter as the proposed test method) [16].

From detailed measurements of the deformation of cracking surfaces that lead to fracture, the authors have confirmed that, rather than displacement of the diagonal cracked surface, opening in the vertical direction is dominant [5]. Furthermore, it has been reported elsewhere that analysis in which the fracture characteristics of diagonal cracking are made equivalent to mode I cracking characteristics offers comparatively good results with regard to the size effect of shear strength [18]. As a result, in this test, mode I fracture energy is applied to study the size effect on shear strength.

5.2 Evaluation of concrete fracture energy [3]

Fracture energy is evaluated here in accordance with the proposed test method discussed above. Testing is set up to correspond with the shear test described in the earlier part of this paper, with the same three types of concrete materials and mixes (L, M, and U) as shown in **Table 3**.

The results of the fracture energy test are shown in **Table 4**. These values are the averages for 5-8 test specimens of each type. The characteristic length in **Table 4** is the value proposed by Gustafsson and Hillerborg, and is derived according to the following formula using the fracture energy G_f resulting from the test [3]:

$$\begin{aligned}
 l_{ch} &= 1000 E_c \cdot G_f / f_t^2 \\
 &= G_f / (2 \cdot 1/2 \cdot f_t \cdot f_t / 1000 E_c) = G_f / 2G_e
 \end{aligned}
 \tag{6}$$

Where G_e is the elastic energy per unit of volume stored in the member until crack propagation. In general, the smaller the characteristic length, the more brittle the fracture becomes. From the test results, as compressive strength increases, the characteristic length decrease, the compressive strength rises, and the more likely it becomes that brittle fracture will occur. If the damage is localized, the total amount of energy released as damage progress (in other words, the energy required to cause fracture) is reduced. This corresponds well with the fact that the characteristic length is reduced as the strength of the concrete increases. Since this means that characteristic length can lead to quantitative evaluation of damage localization (in other words, the tendency for cracking to be localized), it is a useful indicator for evaluating the size effect of shear strength.

Table 5 Existing test data for investigation

Reference	Level	d (mm)	p_w (%)			f_c (N/mm ²)		f_t (N/mm ²)		E_c (kN/mm ²)		τ_c (N/mm ²)		
No.19	L	300	1.23	1.26	24.8		2.29		20		1.13	1.00		
	L	500	1.35			27.3		2.27		21.8		0.98	1.20	
	L	950	1.22			20.7	20.6	1.87	2.00	17.6	17.4	0.70	0.77	
No.20	M	350	1.19			55.1	70.4	3.99	4.02	30.1	34.3	1.62	1.61	
	U	350	1.19			82.5		4.02		36.7		1.75		
	U	550	0.76			84.3		4.71		35.9		1.31		
	U	750	0.55			87.2		4.00		36.8		0.98		
	M	950	1.10			76.5		3.83		37.4		1.01		
No.21	L	150	2.65			32.4		2.75		28.7		1.52	1.47	
	L	150	2.65			38.3		3.14		30.5		1.63	1.52	
	M	150	2.65			48.6		3.47		32.7		1.64	1.79	
	M	150	2.65			70.9		5.14		36.9		1.85	1.88	
	U	150	2.65			83.4		5.52		37.5		2.12	2.36	
	U	150	2.65			128		7.84		42.7		1.91	1.89	
	U	225	2.55			125		7.82		42.3		1.63	1.54	
	U	300	2.58			128		7.84		42.7		1.44	1.27	
No.22	U	150	1.27			90.6		4.91		43.2		2.01		
	U	350	1.23	0.54	0.85	95.5		5.36		43.2		1.44	1.49	1.45
	U	550	1.06			107		6.08		43.2		1.22		
	U	650	0.89			108		6.73		43.2		1.01		

Notice : E_c of reference No.20 show inference values by Eq.(7).

τ_c gives the value converted to a tension reinforcement ratio of $p_{w0} = 1.53\%$.

5.3 Derivation and verification of shear strength calculation formulas

Based on the results given in the preceding paragraph, a study of the size effect of shear strength is carried out on the basis of the characteristic length as obtained from the fracture energy tests, and this leads to the derivation of shear strength calculation formulas.

a) Approach to size effect using fracture mechanics

Studies of the size effect were implemented for cases where the shear span ratio was 3. To improve the accuracy of the study results, the 27 data points are combined with 34 previously reported data points for shear span ratio (Table 5). All of these existing data points were for case with no shear reinforcement and two-point or one-point centralized loading. Regarding the shear strength τ_c in Table 5, since the tensile reinforcement ratio was different for each data point, in accordance with Eq.(4), the shear strength obtained in the test was multiplied by an offset coefficient for the tensile reinforcement $(p_{w0}/p_w)^{1/3}$ to normalize the values to the same $p_{w0} = 1.53\%$ tensile reinforcement ratio as in the cases effective depth 250 mm and 500 mm in this study.

Regarding Young's modulus, which was not clearly indicated in the existing data, estimated values are shown. For $f'_c \leq 80$ N/mm², these estimates were derived through linear interpolation of the values [1] in the Standard Specification for Design and Construction of Concrete Structures. For $f'_c > 80$ N/mm², the estimates were derived from a formula by Tomozawa et al. [23] given as Eq.(7).

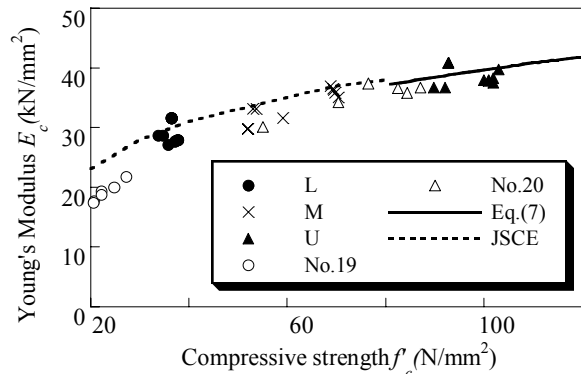


Fig.9 Investigation of Young's modulus

Table 6 Applied fracture energy to investigation of the size effect

f'_c (N/mm ²)	G_f (N/mm)	l_{ch} (mm)
L	~ 45	540 ~ 945
M	45 ~ 80	280 ~ 617
U	80 ~	151 ~ 521

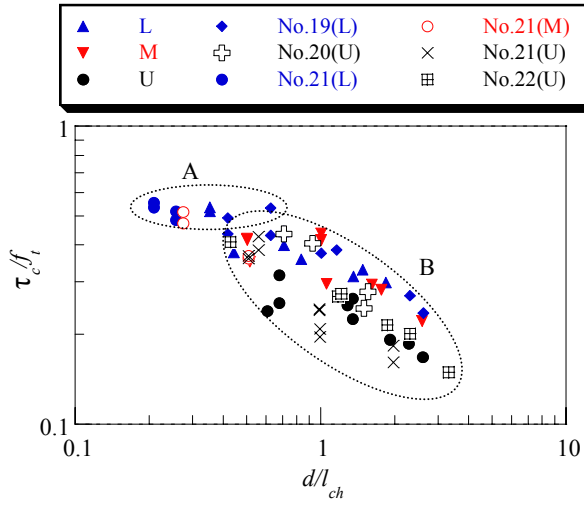


Fig.10 Relation of d/l_{ch} to τ_c / f_t

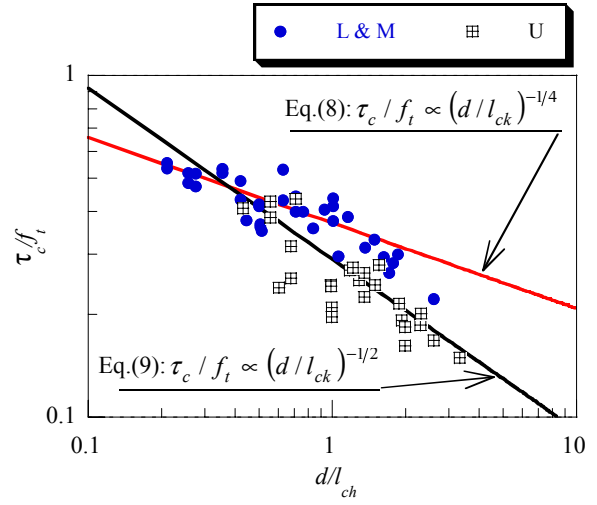


Fig.11 Investigation of size effects

$$E_c = 9.2 \cdot (100 \cdot f'_c / 9.8)^{0.3} \cdot (\gamma / 1000)^2 \times 9.8 / 100 \quad (7)$$

Concrete density γ was set at 2,346 kg/m³ [20]. Regarding the relationship between compressive strength and Young's modulus, **Fig. 9** compares the relationship between estimates in this test and the existing data. From this relationship, the measurements and estimates were judged to be generally in agreement, and the Young's modulus values were evaluated as valid.

As the fracture energy was unknown in the case of the existing data (**Table 5**), the measurements in **Table 4** were divided into three categories according to compressive strength and applied (**Table 6**) to determine the characteristic length values.

As already noted, Gustafsson and Hillerborg have reported that, with regard to the size effect on the shear strength of ordinary-strength concrete, τ_c / f_t is proportional to the minus 1/4 power of d / l_{ch} [3]. With regard to the tendency toward cracking localization, which is conjectured to be a cause of the size effect of shear strength, attention in this study focuses on characteristic length, which can be evaluated quantitatively, and this approach is applied to the study of the size effect of shear strength carried out using the combined results of the present test (**Table 2**) and the existing data (**Table 5**). The results are shown in **Fig. 10**.

Figure 10 confirms that there is a correlation between d / l_{ch} and τ_c / f_t , as in the research by Gustafsson and Hillerborg. The data points for concrete of low- and medium- strength (L and M) are distributed between both grouping A and B marked in **Fig. 10**. In contrast, data points for high-strength concrete (U) fall almost entirely in grouping B. This also indicates that the size effect in high-strength concrete tends to be different from that in low- and medium- strength concrete.

Figure 11 shows the same correlation as in **Fig. 10**, but with the data points plotted as either low- and medium-strength concrete (L and M) or as high-strength concrete (U). Regression analysis for the d / l_{ch} and τ_c / f_t correlations shows that the size effect is almost exactly proportional to d / l_{ch} to the minus 1/4 power and d / l_{ch} to the minus 1/2 power, respectively, for the two cases. Accordingly, these values are adopted, and relational expressions are determined for each using the least squares method. In **Fig. 11**, the red line indicates the curve of Eq.(8), while the black line indicates the curve of Eq.(9).

$$\tau_c / f_t \propto (d / l_{ch})^{-1/4} \quad (8)$$

$$\tau_c / f_t \propto (d / l_{ch})^{-1/2} \quad (9)$$

The test results for low- and medium- strength concrete are expressed by Eq.(8), and this is shown to be in agreement with the existing size effect law (proportional to the effective depth to the minus 1/4 power) as incorporated into the JSCE formula. The test results for high-strength concrete clearly show a different tendency from that represented by Eq.(8), with τ_c/f_t proportional to d/l_{ch} to the minus 1/2 power. In other words, that shear strength is proportional to the effective depth to the minus 1/2 power.

The results of this fracture mechanics based study demonstrated that characteristic length could be used to evaluate the size effect of shear strength in high-strength concrete using the expression giving by Eq.(9). In the next section, based on these results, a formula for calculating shear strength in high-strength concrete will be derived and verified.

b) Derivation and verification of formula to calculate shear strength in high-strength concrete

In order to evaluate shear strength in a rational manner, appropriate values must be established for the size effect and various factors affecting shear strength. Equation (4) by Niwa et al., which was the basis for the JSCE formula, is the product of factors relating to compressive strength, tension reinforcement ratio, effective depth, and shear span ratio. For ordinary-strength concrete, this formula yields results that agree closely with the test results [2]. Accordingly, it was decided to derive a formula for calculating shear strength by considering the various factors also as the product of individual factors.

We consider first the effect of tension reinforcement ratio and shear span ratio. It has been reported as noted above that the tension reinforcement ratio factor for the shear strength of high-strength concrete is no different from that of ordinary strength concrete evaluated using Eq.(4) [13]. As regards the effect of shear span ratio, it was confirmed in Section 4 (4) in that the relationship between shear strength and shear span ratio is not dependent on compressive strength and can be evaluated from the factors relating to shear span ratio in Eq.(4). Accordingly, the relationship between shear strength τ_c and the offset value for shear strength τ_c^* , from which the effects of tension reinforcement ratio and shear span ratio have been eliminated, can be expressed by the relation given below.

$$\tau_c^* = \tau_c / \left\{ (100 p_w)^{1/3} \cdot (0.75 + 1.4/(a/d)) \right\} \quad (10)$$

Next, let us turn to the effect of compressive strength and effective depth. The data used in the study of size effect in the previous section were constant in terms of shear span ratio (which was 3), so the data points show no effect of shear span ratio. Moreover, as corrections were made for differences in tension reinforcement ratio, there is thought to be almost no effect of tension reinforcement ratio. Accordingly, the data points in the study are thought to be almost completely controlled by material properties (of which compressive strength is a typical example) and effective depth. The effect of effective depth is none other than the size effect, so the results of the previous section (Eq.(9)) can be applied.

In the CEB-FIP Model Code 90 [8], the fracture energy is given by the formula below as the relationship between concrete compressive strength and maximum aggregate size.

$$G_f = G_{f0} (f'_c / f'_{c0})^{0.7} \quad (11)$$

Where, G_{f0} : Basic value of fracture energy dependent on maximum aggregate size, f'_{c0} : 10 N/mm², and $f'_c \leq 80$ N/mm².

This study, which is concerned with high-strength concrete where $f'_c > 80$ N/mm², falls outside the scope of this formula. However, the fracture energy in high-strength concrete is also thought to depend on compressive strength, and here the fracture energy in high-strength concrete is postulated in terms of the formula below.

$$G_f \propto f'_c{}^{m_1} \quad (12)$$

where m_1 is a constant. From the relationship between Eq.(7) and Eq.(12), the following relationship results :

$$E_c \cdot G_f \propto (f'_c)^{0.3} \cdot (f'_c)^{m_1} \propto f'_c{}^{m_2} \quad (13)$$

Where m_2 is a constant. If, as a result of this formula, a proportional constant n is introduced into Eq.(9) from Eq.(6) and Eq.(13), the result is as follows:

$$\begin{aligned} \tau_c^* &= n \cdot f_t \cdot \left(d \cdot f_t^2 / E_c \cdot G_f \right)^{-1/2} \\ &= n \cdot f'_c{}^m \cdot d^{-1/2} \end{aligned} \quad (14)$$

This formula enables τ_c^* to be expressed as a relationship between compressive strength and effective depth (in which m is a constant). As a result, it is possible to evaluate shear strength using effective depth and, as a material property, compressive strength.

Next, from among the results of this test (**Table 2**) and the existing data (**Table 5**), let us take the data points for high-strength concrete ($f'_c > 80 \text{ N/mm}^2$) to determine the relationship between constants n and m (in other words, $\tau_c^*/d^{1/2}$ and f'_c). **Figure 12** shows the relationship between $\tau_c^*/d^{1/2}$ and f'_c . The results of regression analysis (the line in the figure) are shown below.

$$\tau_c^* / d^{-1/2} = 190 f'_c{}^{-0.51} \quad (\text{Correlation } 0.66)$$

Furthermore, the above formula can be used to simplify Eq.(15) in a practical manner, as indicated by the broken line in **Fig. 12**.

$$\tau_c^* / d^{-1/2} = 180 f'_c{}^{-1/2} \quad (\text{Correlation } 0.66) \quad (15)$$

It can be seen from **Fig. 12** that the results given by Eq.(15) are in almost perfect agreement with the regression analysis, and that there is comparatively good correlation between compressive strength and $\tau_c^*/d^{1/2}$. Accordingly, Eq.(14) can be expressed as follows:

$$\tau_c^* = 180 f'_c{}^{-1/2} \cdot d^{-1/2} \quad (16)$$

As is clear from Eq.(16), the material property factors in the shear strength of high-strength concrete are evaluated using $f'_c{}^{-1/2}$, as opposed to those for ordinary strength concrete which are evaluated using $f'_c{}^{-1/3}$.

From the above, the following formula is proposed as a formula for calculating the shear strength of high-strength concrete (compressive strength $80 < f'_c \leq 125 \text{ N/mm}^2$).

$$\begin{aligned} \tau_c &= \tau_c^* \cdot (100 p_w)^{1/3} \cdot (0.75 + 1.4/(a/d)) \\ &= 180 f'_c{}^{-1/2} \cdot d^{-1/2} \cdot (100 p_w)^{1/3} \cdot (0.75 + 1.4/(a/d)) \end{aligned} \quad (17)$$

To verify the accuracy of Eq.(17) for a shear span ratio of 3 and a tensile reinforcement ratio of 1.53% a comparison of the results of this test (**Table 2**) and existing research data (**Table 5**) corresponding to compressive strengths of 80, 90, 100, and 125 N/mm^2 , is shown in **Fig.13**, with calculations of shear strength using each of the compressive strength values. **Figure 13** shows the test results for a tension reinforcement ratio of 1.53% and for offset values with the tension reinforcement ratio converted to 1.53%. With the effective depth for each compressive strength value as a parameter, this figure shows results obtained with

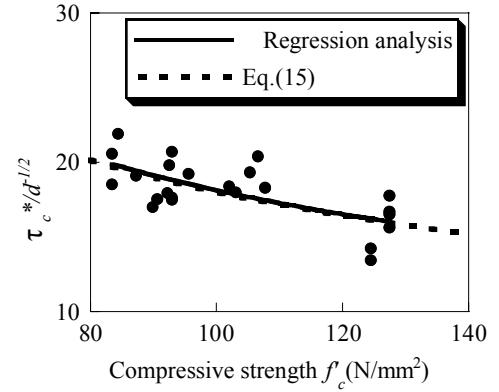


Fig.12 Relation of constants n and m to compressive strength

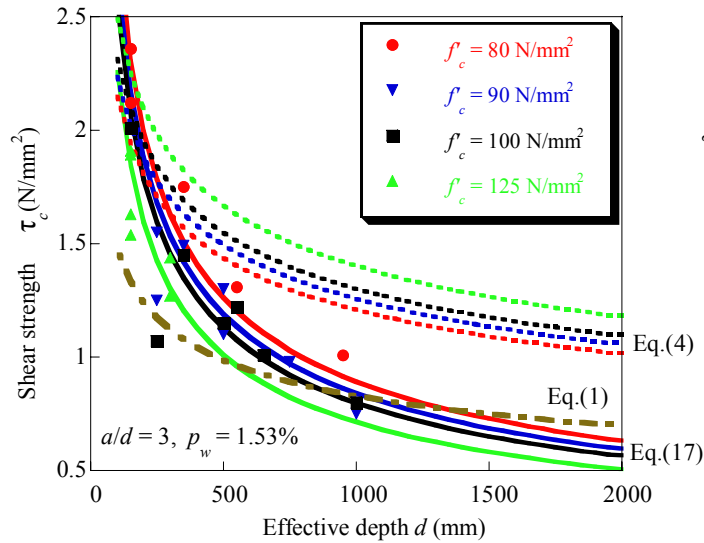


Fig.13 Comparison of the proposed formula with test results

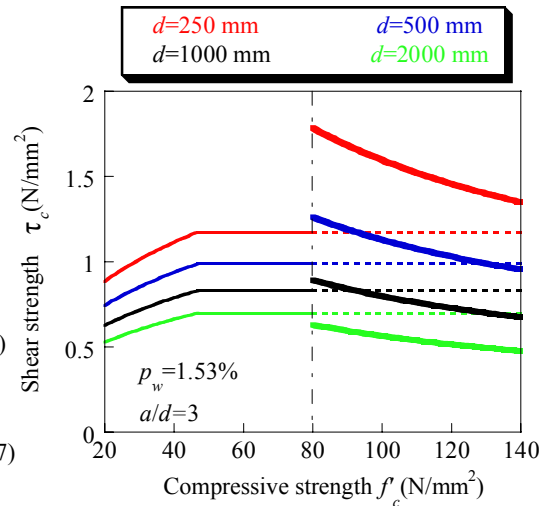


Fig.14 The relation of Eq.(1) to Eq.(17) at $f'_c = 80 \text{ N/mm}^2$

Eq.(17) as solid lines and those obtained with Eq.(1) (the JSCE formula) and Eq.(4) as the dashed line and the dotted lines, respectively. From **Fig. 13**, it can be seen that the results obtained with Eq.(1) fall generally in the safe zone for compressive strengths 80 – 100 N/mm² and effective depths less than 1,000 mm. In particular, when the effective depth is small, the shear strength tends to be evaluated on the low side; conversely, as the effective depth becomes larger, the safety factor with respect to the test results tends fall.

It has been thought that Eq.(1) can also be applied to high-strength concrete as long as a suitable safety coefficient is employed. However, these results demonstrate that it is not rational to set a uniform safety coefficient, and thorough consideration is required particularly in applications to structures with large member sizes.

It can also be seen that Eq.(17) accurately matches the test results, and that the formula maintains the same accuracy throughout the compressive strength ranges of 80 - 125 N/mm² and the effective depths range of 150 - 1,000 mm. In other words, Eq.(17) provides a valid evaluation of the size effect of high-strength concrete and enables a rational assessment of shear strength based on the special characteristics of high-strength concrete. Moreover, comparisons of the test results for high-strength concrete with a shear span ratio of 3 (26 data points) in **Table 2** and **Table 5** with the results of calculation using Eq.(1) and Eq.(17) reveal that the average value of the ratio for the former is 1.27 with a coefficient of variation of 17.5%, while the average ratio for the latter is 1.01 with a coefficient of variation of 11.3%. Similarly, a comparison of the cases in which diagonal tensile failure occurred regardless of shear span ratio (31 data points) and calculations carried out with Eq.(17) reveals that the average value of the ratio is 1.01 with a coefficient of variation of 10.7%, demonstrating that Eq.(17) retains the same accuracy even when the shear span ratio differs.

Nevertheless, Eq.(17) is an empirical formula based on test data. At this stage, it would be difficult to say that there is sufficient test data on fracture energy and shear for high-strength concrete in the range of large member. Accordingly, it is thought that, in applying when Eq.(17) to actual design, the safety coefficient should be set on the high side so as to ensure that the calculated results fall within the safe zone. Further studies based on data accumulated in the future will further improve the accuracy of Eq.(17).

Finally, **Fig. 14** compares calculations of the relationship between shear strength and compressive strength carried out using the existing Standard Specification for Design and Construction of Concrete Structures (Eq.(1)) and the proposed formula (Eq.(17)). In the case of the Standard Specification calculation, a solid line is used to show results within the applicable range ($f'_c \leq 80 \text{ N/mm}^2$), while a dotted line indicates results outside this range. For the proposed formula, a thick line is used to show the applicable range ($f'_c > 80 \text{ N/mm}^2$). Here the tension reinforcement ratio is 1.53% and the shear span ratio is 3. These results show that, for reinforced concrete beams with no shear reinforcement and an effective depth of 1,000 mm or less

(which were the subject of this study) the values given by the proposed formula are greater than those given by the Standard Specification at 80 N/mm^2 , the boundary between the applicable ranges. However, this difference between the results falls as the effective depth is increased, and situation is reversed at an effective depth of 1,340 mm; at the point, the values given by the proposed formula are less than those given by the Standard Specification. Accordingly, within the range of this verification, the existing Standard Specification formula provides values on the safe side, but in the case of large sizes members that are outside the range of verification, there is a possibility that the evaluation will be too great. The continuity of these assessment formulas should be a topic for future study.

6. CONCLUSION

In this study, shear tests were conducted on reinforced concrete beams without shear reinforcement and with compressive strengths in the range $36 - 100 \text{ N/mm}^2$, effective depths of $250 - 1,000 \text{ mm}$, and shear span ratios of $2 - 5$. This aim was to study shear strength and the size effect of shear strength. Existing research data was also used to create a proposal for the shear strength assessment of high-strength concrete, basing the effort on a study of the size effect using fracture mechanics. The conclusions drawn from this study can be summarized as follows:

- (1) In the shear failure of reinforced concrete beams without shear reinforcement, the greater the effective depth and the greater the compressive strength, the more significant the localization of cracking became, while at the same time the size effect became more significant.
- (2) A study of the size effect of shear strength using characteristic length based on fracture mechanics revealed that, for low- and medium-strength concrete, the shear strength was proportional to effective depth to the minus $1/4$ power, as reported in other research results. For high-strength concrete, however, the shear strength was confirmed to be proportional to the effective depth to the minus $1/2$ power.
- (3) The material properties factor in the shear strength of high-strength concrete was evaluated using $f_c^{-1/2}$, unlike ordinary strength concrete, which is evaluated using $f_c^{1/3}$.
- (4) Based on the test results for compressive strengths $80 < f_c \leq 125 \text{ N/mm}^2$, Eq.(17) was proposed as a formula for assessing the shear strength of reinforced concrete beams made with high-strength concrete without shear reinforcement. The prediction accuracy of this formula was confirmed to be very high; for 31 test specimens with compressive strengths in the range $80 < f_c \leq 125 \text{ N/mm}^2$ and effective depths of up to 1,000 mm, the average was ratio to the test results was 1.01, with a coefficient of variation of 10.7%.

7. A FINAL NOTE

This research focused on a study of the shear strength of high-strength reinforced concrete beams without shear reinforcement. For reinforced concrete beams with shear reinforcement, it has been reported that the self-compression of high-strength concrete is greater than that of ordinary-strength concrete, and the resulting internal stress and initial defects reduces shear strength [24]. Further, this study was based on the results of shear tests conducted on reinforced concrete beams made with high-strength concrete and with a tension reinforcement ratio of approximately $p_w = 1.5\%$. As no detailed studies of the effect of tension reinforcement ratio have been performed, this reinforcement ratio was adopted in accordance with the work carried out by Niwa et al., who studied ordinary-strength concrete. The amount of tension reinforcement will affect the internal stress resulting from self-compression of the high-strength concrete. Thus, in future, further studies must be carried out to determine the shear strength characteristics of reinforced concrete beams made of high-strength concrete, focusing on the effect of internal constraints such as shear reinforcement, tension reinforcement, etc.

References

- [1] JSCE, "Standard Specification for Design and Construction of Concrete Structure, Design", 1996.
- [2] Niwa, J., Yamada, K., Yokozawa, K. and Okamura, H., "Reevaluation of the Equation for Shear Strength of Reinforced Concrete Beams without Web Reinforcement", Proceedings of the JSCE, No.372/V-5, pp.167-176, 1986. (in Japanese)
- [3] Gustafsson, P. J. and Hillerborg, A., "Sensitivity in Shear Strength of Longitudinally Reinforced Concrete Beams to Fracture Energy of Concrete", *ACI Structural Journal*, May-June, pp.286-294, 1988.
- [4] Fujita, M., Oodate, T., Yasuda, T. and Sato, R., "Experimental Study on Size Effect of High-strength concrete Beams", Proceedings of JCI, vol.20, No.3, pp.349-354, 1998. (in Japanese)
- [5] Fujita, M., and Oodate, T., "Effect of Concrete Strength on Shear Fracture Yield Strength in Concrete Beam Members", Proceedings of JCI, vol.33, pp.955-960, 2000. (in Japanese)
- [6] Fujita, M., Oodate, T., and Matsumoto K., "Influence of Fracture Energy on Size Effect in Shear Strength of RC Beams", Proceedings of JCI, vol.23, No.3, pp.751-756, 2001. (in Japanese)
- [7] American Concrete Institute, "ACI Manual of Concrete Practice Part 3", 1999.
- [8] CEB-FIP, "Model Code 1990, Comite Euro-International du Beton", Buelletin D'Information No.213/214, Lausanne
- [9] Bazant, Z. P., and Kim, J-K., "Size Effect in Shear Failure of Longitudinally Reinforced Beam", *Journal of ACI*, Sept.-Oct., pp.456-468, 1984.
- [10] Okamura, H., and Higai, T., "Proposed Design Equation for Shear Strength of Reinforced Concrete Beams without Web Reinforcement", *Proc. of JSCE*, No.300, pp.131-141, August 1980.
- [11] Iguro, M., Shioya T., Nojiri Y., and Akiyama, H., "Experimental Studies on the Shear Strength of Large Reinforced Concrete Beams under Uniformly Distributed Load", Proceedings of the JSCE, No.348/V-1, pp.175-184, 1980. (in Japanese)
- [12] JCI, "JCI Colloquium on Fracture Mechanics of Concrete Structures Part I (Committee Report), 1990. (in Japanese)
- [13] Suzuki, M., Ozaka, Y. and Imafuku, K., "Shear Characteristics of Ultra High-strength concrete Beam without Shear Reinforcement", *JCA Proceedings of Cement & Concrete*, No.47, pp.558-563, 1993. (in Japanese)
- [14] An, X., Maekawa, K. and Okamura, H., "Numerical Simulation of Size Effect in Shear Strength of RC Beams", *J. Materials Conc. Struct., Pavement; JSCE*, No.564/V-35, pp.297-316, 1997.
- [15] An, X., and Maekawa, K., "Numerical Simulation on Shear Failure of RC Beams", *Fracture Mechanics of Concrete Structures, Proceedings FRAMCOS-3*, pp.1419-1428, 1998.
- [16] JCI, "Report of JCI Technical Committee on Test Method for Fracture Property of Concrete", 2001. (in Japanese)
- [17] JCI, "Applications of Fracture Mechanics to Concrete Structures", 1993. (in Japanese)
- [18] Niwa, J., Nasra, Z., and Tanabe, T., "Size Effect Analysis for Shear Strength of Concrete Beams Based on Fracture Mechanics, Proceedings of the JSCE", No.508/V-26, pp.45-53, 1995. (in Japanese)
- [19] Public Works Research Institute, "Report on shear loading test data of large scale RC beams", Technical Memorandum of PWRI, No.3426, 1996. (in Japanese)
- [20] Public Works Research Institute, "Joint Research on Design Method of High-strength Concrete Structures- Study on shear strength of PC beams with High-strength concrete", Cooperative Research Report of PWRI, No.122, 1995. (in Japanese)
- [21] Matsui, Y., Uchida, Y., Rokugo, K., and Koyanagi, W., "Shear strength of Reinforced High-strength concrete Beams without Stirrups", Proceedings of JCI, vol.17, No.2, pp.655-660, 1995. (in Japanese)
- [22] Abe, Y. Ito, K., Matsubara, K., and Suzuki, M., "An Experimental Study on Shear strength of Reinforced Concrete Beams without Shear Reinforcement Using Ultra High Strength Materials", Proceedings of JCI, vol.21, No.3, pp.181-186, 1999. (in Japanese)
- [23] Tomozawa, F., Noguchi, T., and Onoyama, K., "Investigation of Fundamental Mechanical Properties of High Strength and Super High-strength concrete", Summaries of Technical Papers of Annual Meeting Architectural Institute of JAPAN, pp.497-498, 1990. (in Japanese)
- [24] Hayakawa, T., Fujita, M., Mise, A., and Sato, R., "Effects of Shrinkage of High-strength concrete on the Strain Behavior in Shear Reinforcement", Proceedings of JCI, vol.22, No.3, pp.589-594, 2000. (in Japanese)